Electronic Supplementary Material (ESI) for RSC Advances.

Tunable multilayer assemblies of nanofibrous composite mats as permeable protective materials against chemical warfare agents

Su-Yeol Ryu, Jae Woo Chung,* and Seung-Yeop Kwak*

Supporting Information

Table S1: Mechanical properties of pristine polyamide 66 nanofiber (PANF) and composite nanofiber mats ([I]MgO/PANF and [I]POM/PANF).

	Modulus (N/mm^2)	Tensile stress at yield (MPa)	Tensile strain at yield (%)	Tensile stress at break (MPa)	Tensile strain at break (%)
PANF	209.51 ± 13.73	5.23 ± 0.20	2.45 ± 0.18	25.47 ± 1.07	42.10 ± 1.74
[I]MgO/PANF	253.07 ± 21.42	6.52 ± 0.04	2.09 ± 0.25	24.62 ± 1.95	36.09 ± 1.86
[I]POM/PANF	228.94 ± 19.54	4.64 ± 0.01	2.10 ± 0.01	18.86 ± 0.97	41.79 ± 1.54

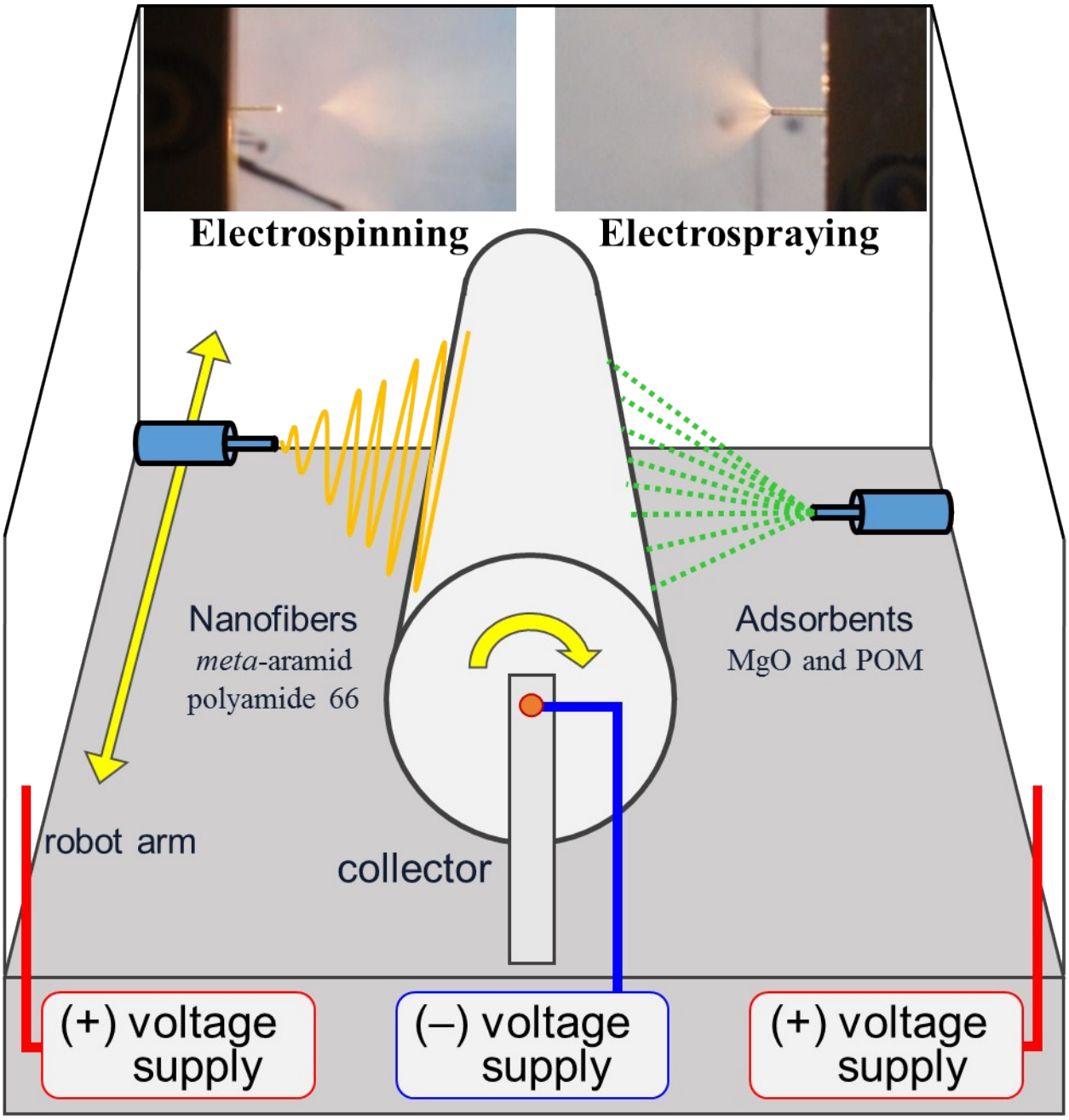

Figure S1: Schematic representation of the simultaneous electrospinning and electrospraying (SEE) process.

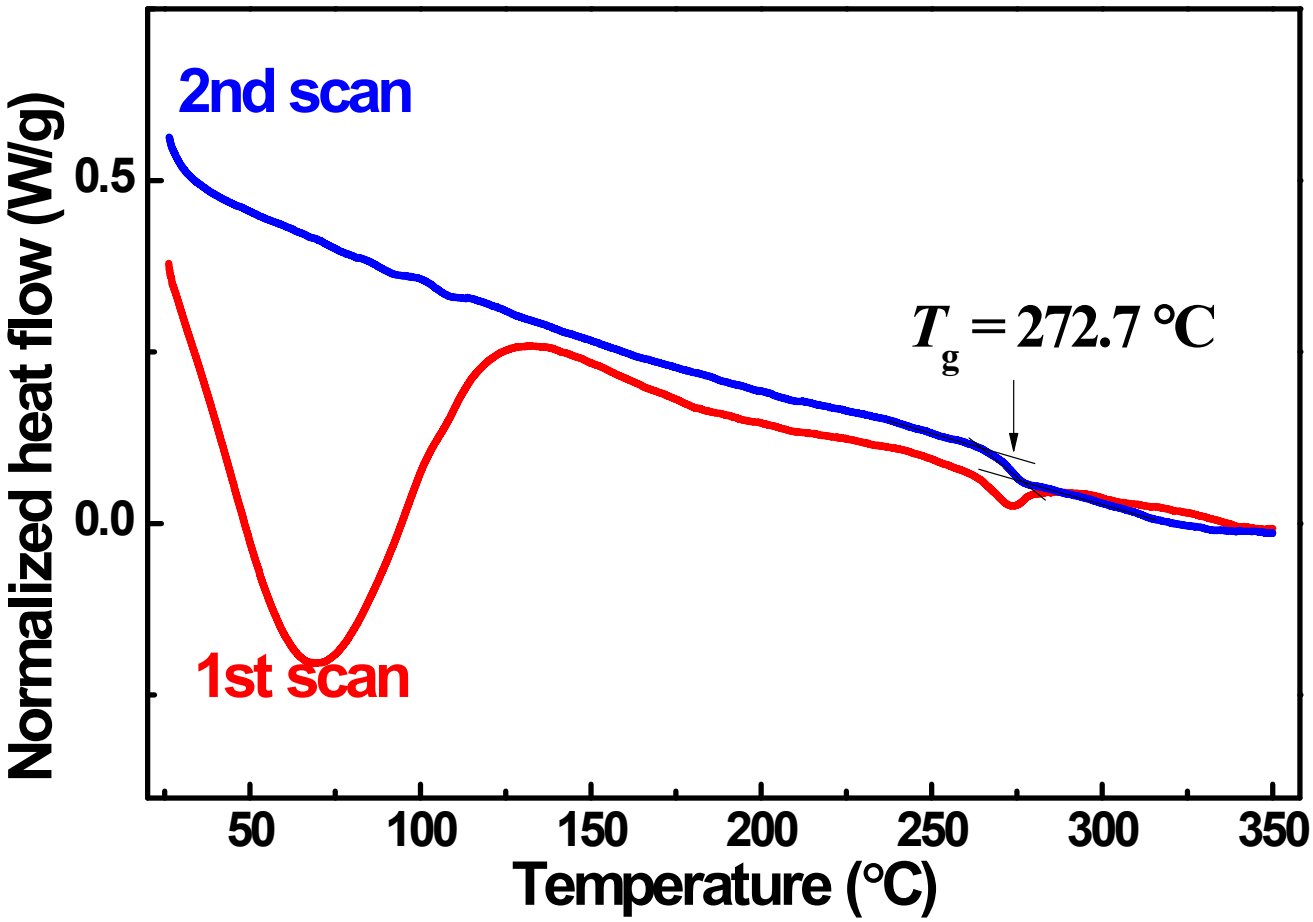

Figure S2: First and second differential scanning calorimetry curves of *m*ANF. The glass transition temperature (T_g) of *m*ANF was detected at around 273 °C.

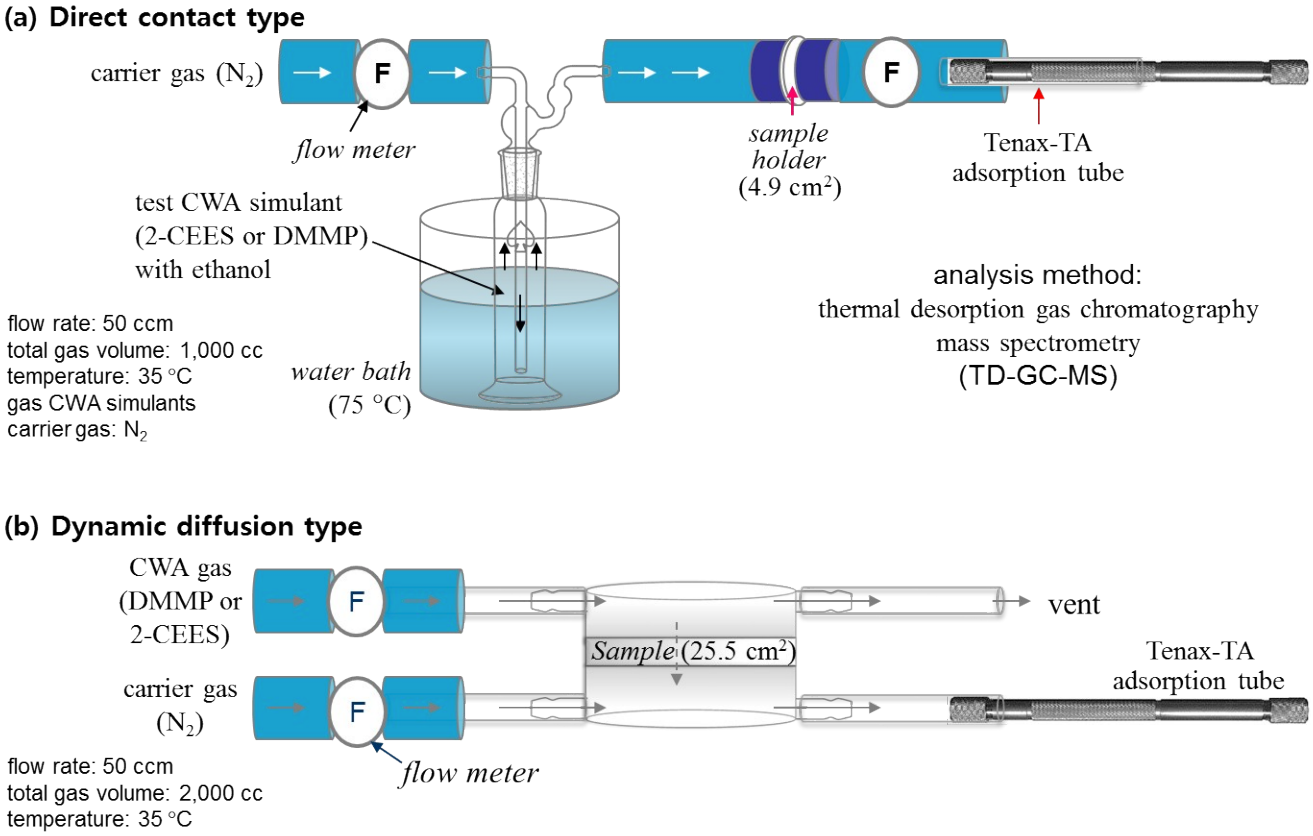

Figure S3: Schematic representations of experimental systems used to investigate the resistance of the composite nanofiber mats to permeation by gas CWA simulants according to a modified ASTM F739 standard.

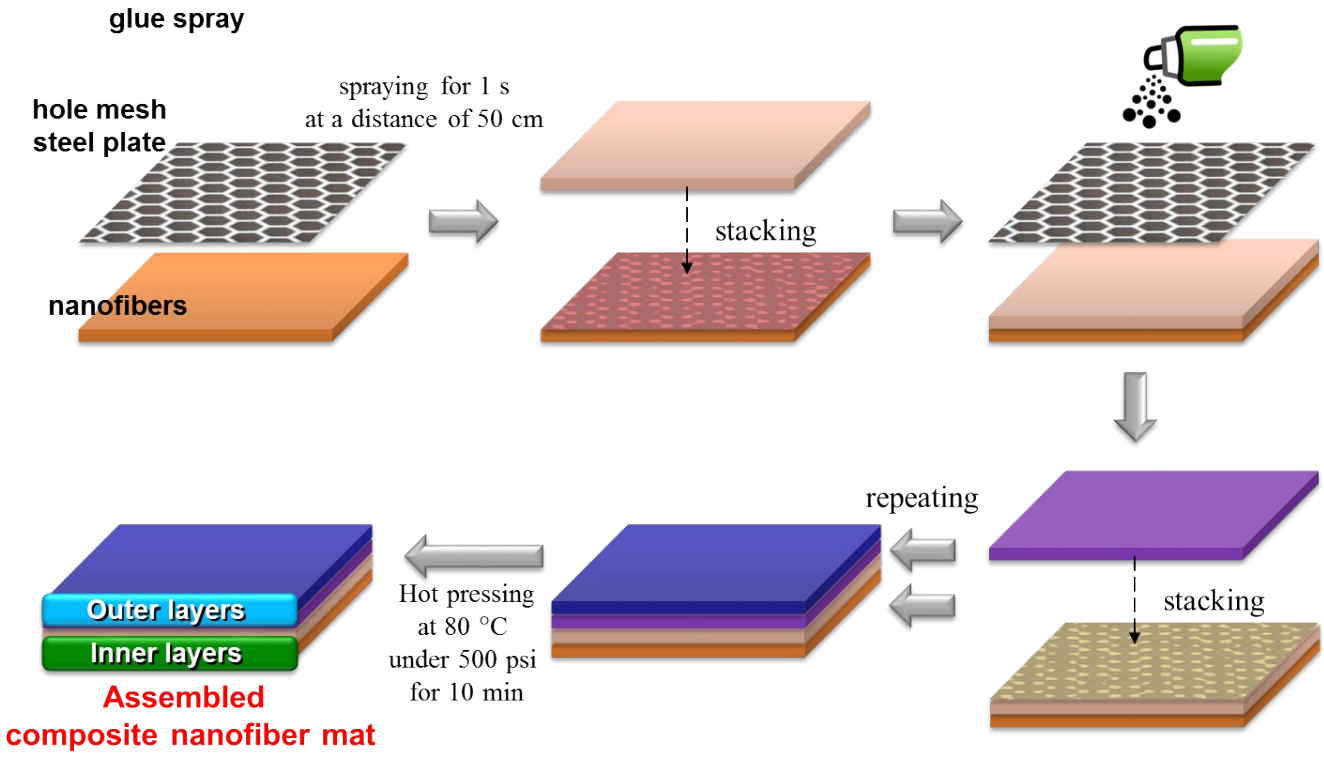

Figure S4: Fabrication of assemblies of composite nanofiber mats *via* adhesion with glue spraying and hot pressing.

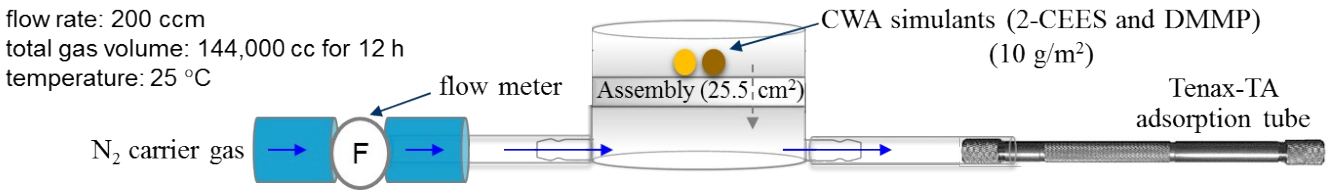

Figure S5: Schematic representation of the permeation experiments performed according to the TOP 8-2-501 standard.

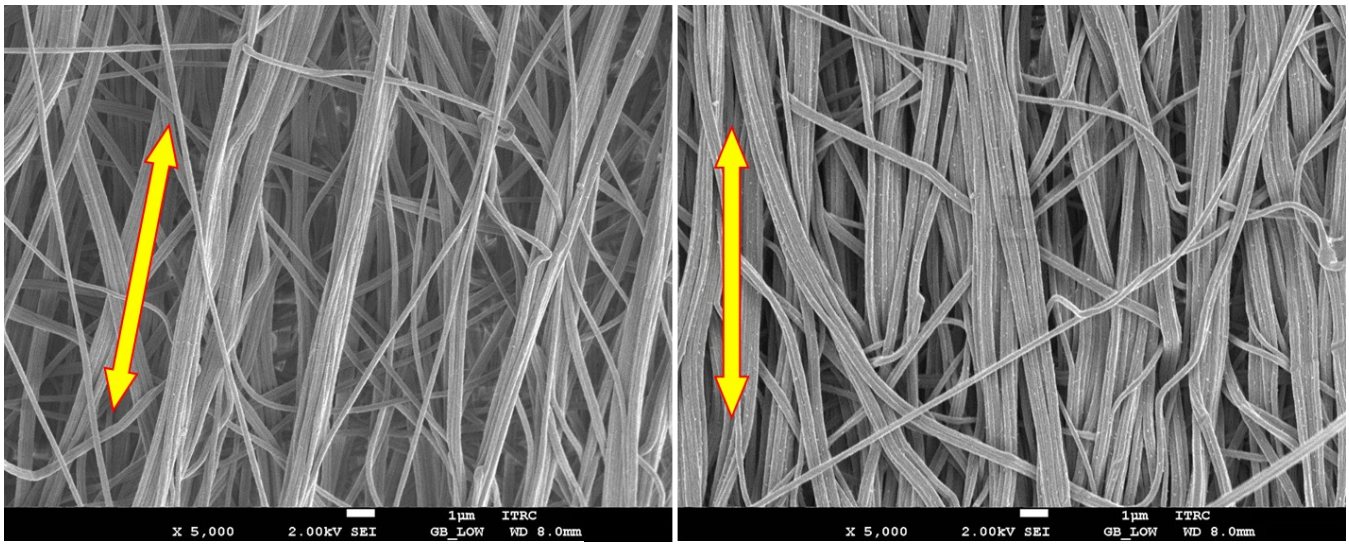

Figure S6: Morphology of pristine *meta*-aramid nanofibers. Double headed arrows show the alignment direction of the *meta*-aramid nanofibers. The scale bar represents 1 μm.

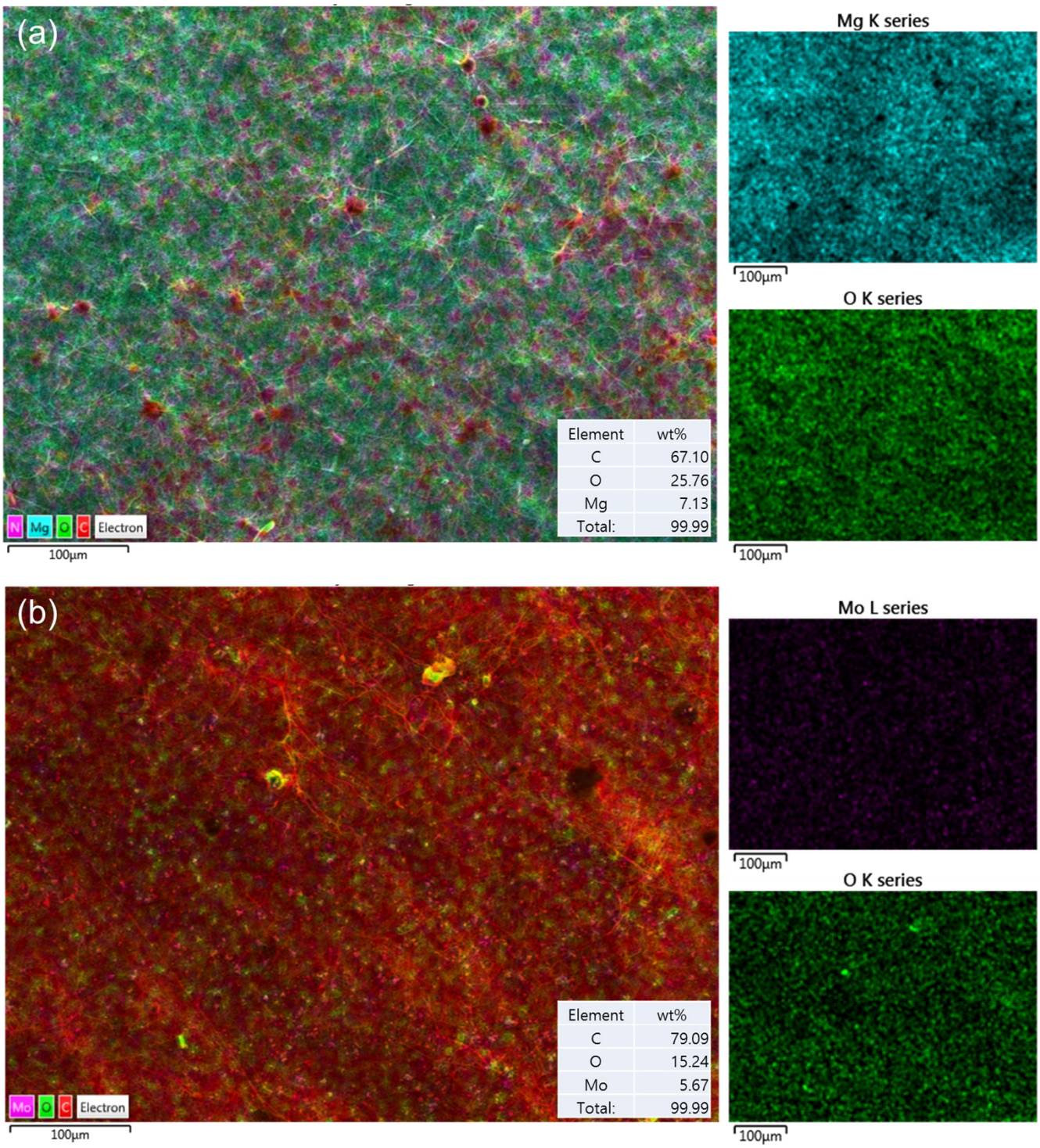

Figure S7: EDS mapping image of (a) MgO/*m*NAF and (b) POM/*m*ANF nanofibre composites.

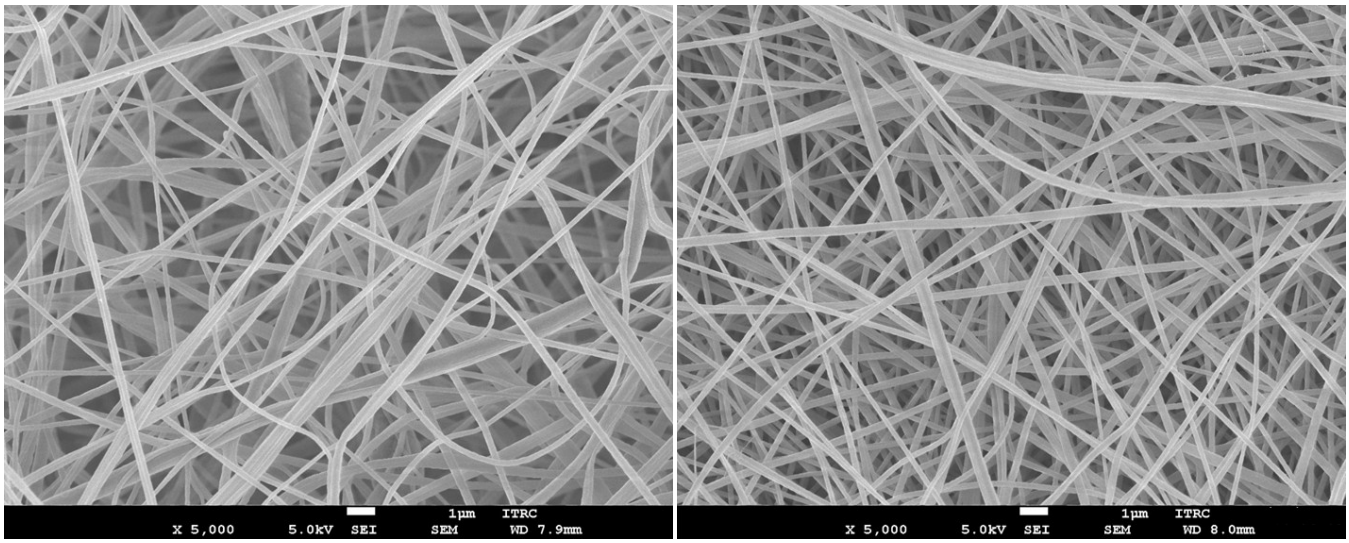

Figure S8: Morphology of pristine polyamide 66 nanofibers. The scale bar represents 1 μm.

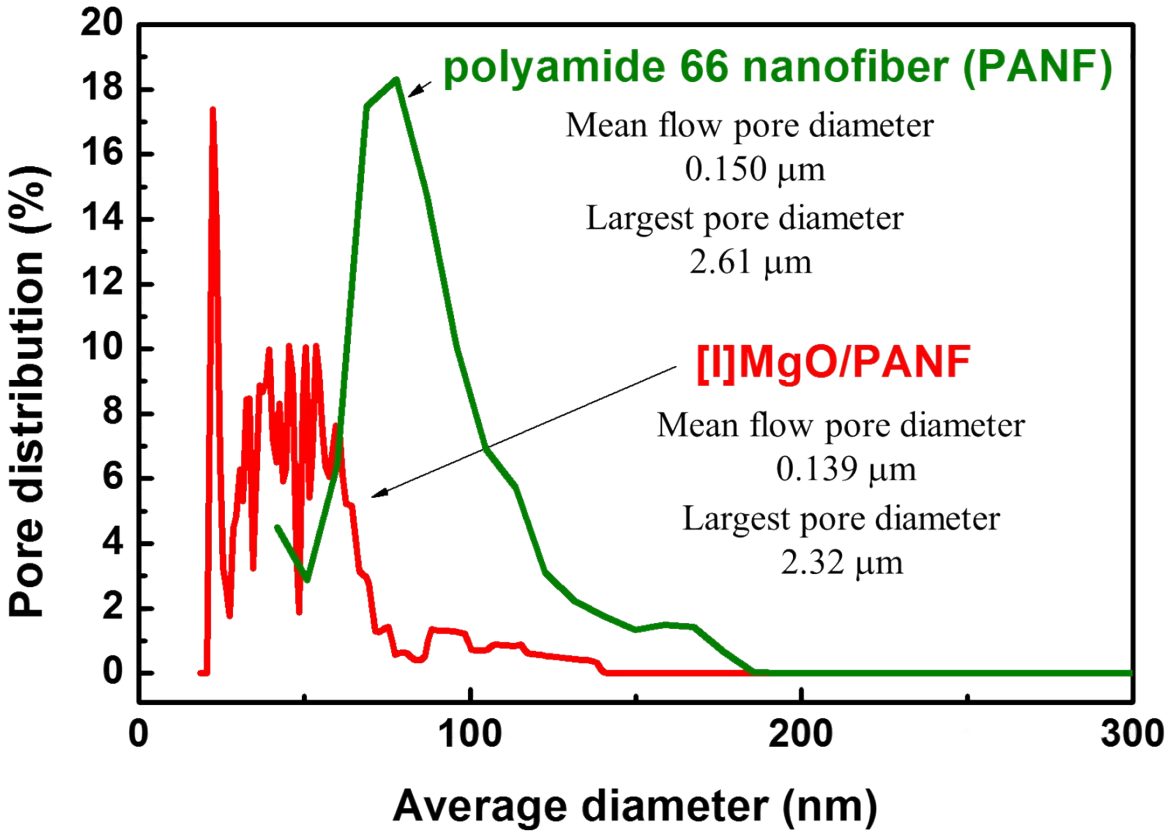

Figure S9: Flow pore characteristics of the nanofiber mats PANF and [I]MgO/PANF measured by capillary flow porometry.

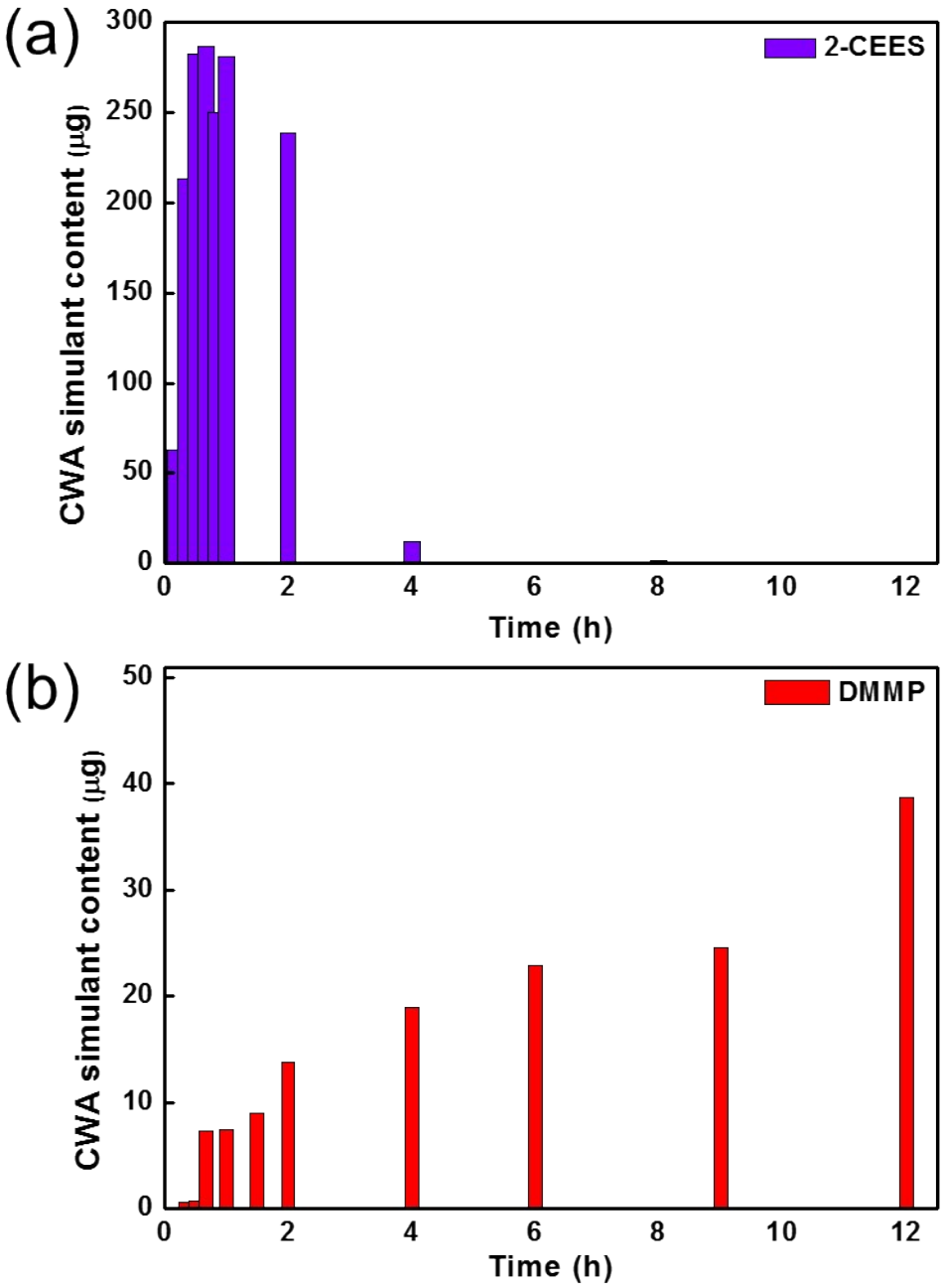

Figure S10: Penetration behavior of CWA simulants through assemblies containing MgO: (a) 2-CEES and (b) DMMP.